frontiers | Frontiers in Energy Research

TYPE Review
PUBLISHED 13 April 2023
DOI 10.3389/fenrg.2023.1135188

OPEN ACCESS

EDITED BY
Hailong Li,
Central South University, China

REVIEWED BY
Shufeng Shen,
Hebei University of Science and Technology, China
Tse-Lun Chen,
ETH Zürich, Switzerland

*CORRESPONDENCE
Sukanta Kumar Dash,
sk.dash@sot.pdpu.ac.in

SPECIALTY SECTION
This article was submitted to Carbon Capture, Utilization and Storage, a section of the journal Frontiers in Energy Research

RECEIVED 31 December 2022
ACCEPTED 17 March 2023
PUBLISHED 13 April 2023

CITATION
Shukla C, Mishra P and Dash SK (2023), A review of process intensified CO_2 capture in RPB for sustainability and contribution to industrial net zero.
Front. Energy Res. 11:1135188.
doi: 10.3389/fenrg.2023.1135188

A review of process intensified CO_2 capture in RPB for sustainability and contribution to industrial net zero

Chetna Shukla[1], Poonam Mishra[1] and Sukanta Kumar Dash[2]*

[1]Department of Mathematics, Pandit Deendayal Energy University, Gandhinagar, Gujarat, India, [2]Department of Chemical Engineering, (CO_2 Research Group) Pandit Deendayal Energy University, Gandhinagar, Gujarat, India

Carbon dioxide (CO_2), a significant greenhouse gas released from power plants and industries, substantially impacts climate change; minimizing it and achieving carbon net zero is essential globally. In the direction of reducing CO_2 emissions into the atmosphere, post-combustion carbon capture from large point CO_2 emitters by chemical absorption involving the absorption of this gas in a capturing fluid is a commonly used and efficacious mechanism. Researchers have worked on the process using conventional columns. However, process intensification technology is required because of the high capital cost, the absorption column height, and the traditional columns' low energy efficiency. Rotating packed bed (RPB) process intensification equipment has been identified as a suitable technology for enhanced carbon capture using an absorbing fluid. This article reviews and discusses recent model developments in the post-combustion CO_2 capture process intensification using rotating packed beds. In the literature, various researchers have developed steady-state mathematical models regarding mass balance and energy balance equations in gas and liquid phases using ordinary or partial differential equations. Due to the circular shape, the equations are considered in a radial direction and have been solved using a numerical approach and simulated using different software platforms, viz. MATLAB, FORTRAN, and gPROMS. A comparison of various correlations has been presented. The models predict the mole fraction of absorbed CO_2 and correspond well with the experimental results. Along with these models, an experimental data review on rotating packed bed is also included in this work.

KEYWORDS

carbon capture, chemical absorption, process intensification, rotating packed bed, process modeling

1 Introduction

The most challenging task currently is to control the increased levels of greenhouse gases (GHGs) in the atmosphere, which leads to global warming. Among the various GHGs, carbon dioxide (CO_2) significantly affects global warming. GHGs are being released into the atmosphere through multiple activities such as fuel combustion, manufacturing, construction, industrial process, transportation, and agriculture. CO_2 emissions from factories and power plants are the most significant sources of atmospheric pollution. Following the International Panel on Climate Change (IPCC) report, the CO_2 level will have increased to 570 ppm in the atmosphere by 2,100. This CO2 level will cause an increase

in global temperature of approximately 1.9°C. (IPCC, 2022). There is a need to reduce these emissions of GHGs, and hence carbon capture, storage, and utilization (CCSU) is a solution. Though various technology options are available, such as pre-combustion, oxyfuel combustion, and post-combustion carbon capture (PCC), post-combustion is the widely preferred method as it can be used in the pre-existing plant compared to the other two methods (Marx-Schubach and Schmitz, 2019). The technologies available for the post-combustion process include membrane separation, solvent absorption, cryogenic fractionation, and adsorption using solid sorbent (Afkhamipour and Mofarahi, 2013; Dey et al., 2018). Chemical absorption is a widely observed post-combustion method used for capturing carbon compared to other techniques due to its high absorption rate (Joel et al., 2014).

The desirable properties of a suitable solvent are high thermodynamic capacity, high absorption rate, low energy for regeneration, less degradation, lower volatility, and lower corrosivity (Dey et al., 2020). Due to its desirable properties, the solvent used in industry is an amine-based solvent such as primary, secondary, tertiary, and sterically hindered amines (H. Li et al., 2013).

For years, researchers have studied post-combustion CO_2 capture through chemical absorption using different solvents in the conventional column. These include aqueous solutions of monoethanolamine (MEA), diethanolamine (DEA), methyl diethanolamine (MDEA), 2-amino-2-methyl-1-propanol (AMP), and blended amine AMP and piperazine. The most widely used alkanolamines in the literature include MEA, DEA, and MDEA (Dash et al., 2012). Currently, many experiments have been conducted using blended amine AMP and piperazine or its derivatives (Dash et al., 2022; M; Wang et al., 2011; Wu et al., 2020). Mathematical models and operational parameters of the conventional absorber have been studied, modeled, and simulated in various research papers (Pandya, 1983; Akanksha et al., 2007; Kvamsdal et al., 2009; Harun et al., 2012; Koronaki et al., 2015; Jin et al., 2019; Shahid et al., 2021). However, the large size of the conventional column has been cited as a hindrance to CO_2 capture. The problems are that it demands significant capital and operating costs, uses a lot of energy, and requires intercooling with heat integration (Chamchan et al., 2017). Thus, more efficient gas-liquid reactors employing new principles and technology for carbon dioxide capture are needed.

Process intensification technology is used to reduce capital costs and significantly improve process dynamics. The equipment can be made smaller using centrifugal forces, electrical fields, and microwaves or by downsizing to the meso- or microscale (Reay, 2008; Cortes Garcia et al., 2017). One of the most cutting-edge intensification technologies invented by Mallinson and Ramshaw (Mallinson and Ramshaw, 1981) is currently the rotating packed bed (RPB). Podbielniak, (1935) introduced the concept of reducing the height of the distillation column and designed a conceptual contactor for distillation. Mallinson and Ramshaw introduced the idea of rotating packed bed columns similar to that proposed by Pilo and Dahlbeck for distillation and absorption (Rao, 2022). The RPB is used in place of a packed bed absorber to capture CO_2 (M. Wang et al., 2015).

An RPB has been designed and installed at our laboratory to make a complete pilot plant for CO_2 capture. The process flow diagram of the RPB shown in Figure 1A, has the appearance of a doughnut, which spins to produce acceleration caused by centrifugal force. This force is far better than the acceleration caused by gravity applicable in conventional absorption columns for the promotion of micromixing and enhanced mass transfer. The spinning packed bed consists of a rotor with packing that has a considerable surface area and is shaped like a doughnut. A schematic diagram of the rotor is presented in Figure 1B. The solvent is first supplied to the rotor's center. It is forced by the rotor force to flow in the circular direction via the space between the packing. Under the influence of the pressure gradient, the gas flow occurs concurrently in the direction opposite to the flow of the solvent. When the shaft is connected to a motor, the rotor may be rotated at high rates, creating significant gravitational acceleration. Using centrifugal force, a liquid distributor may transport the liquid to the packing's inner edge (Ayash and Mahmood, 2022). This enhances the efficiency of mass transfer and is also an essential component of process intensification.

An RPB works on the principle of centrifugal acceleration (a_c), so an increase in (a_c) leads to a higher slip velocity, increasing flooding character and interfacial shear stress. This, in turn, enhances the mass transfer coefficient (Jassim et al., 2007). Due to the stronger centrifugal acceleration compared to gravity, packings having a greater contact area may be utilized, allowing the reactor to run at a higher flooding limit (Dhaneesh and Ranganathan, 2022). Using RPBs rather than packed bed absorbers shows a higher mass transfer rate. This is accomplished by expanding the interfacial area through a droplet, and film flow is attained via rotational motion, which produces a substantial decrease in the dimension and mass of the rigs (Guo et al., 2019). The reduction in the size of an RPB enables it to be built more inexpensively than traditional fixed-bed reactors. (Pan et al., 2017). A conventional column necessitates a substantial packed volume, resulting in higher capital costs. According to M. Wang et al. (2015), an RPB has excellent potential for minimizing operating and capital expenses for CO_2 capture compared to conventional columns. This article provides a detailed review of the current research on intensified post-combustion capture and discusses experimental rigs (intensified absorber, stripper, and heat exchanger), international laboratory research, solvent sampling, and simulated models. RPBs may be used as a highly efficient multiphase contactor due to the gravity created by the rotation of packing, which can approach 5,000 m^{-2}. Using an RPB absorber improves separation efficiency, as demonstrated by Chamchan et al. (2017), and causes a considerable drop in height transfer unit (HTU). It utilizes just 35% of the packed bed absorber volume.

However, RPB equipment is associated with more significant maintenance and repair expenses. Furthermore, the design of an RPB is more complex; design methodologies and relevant models are not as well defined as conventional packed columns. Despite this, an RPB is favored for CO_2 capture over a packed bed column as the HiGee technology has more advantages. Because of an RPB's high-efficiency mass transfer performance and reduction in size in comparison to the conventional column, it has wide industrial applications. These applications are selective removal of H2S, desulphurization, dedusting, and deaeration of water, as well as an application in the pharmaceutical industry where higher purity of a product is required (Neumann et al., 2018).

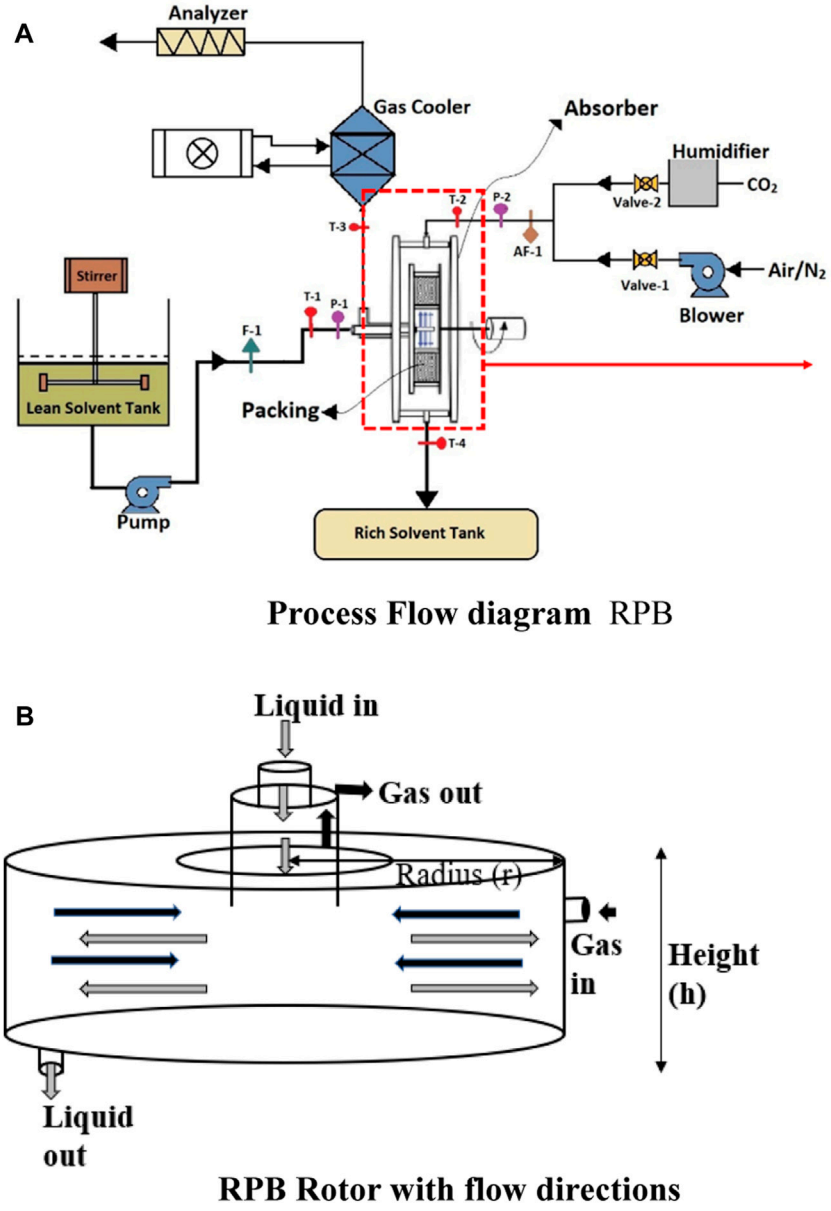

FIGURE 1
(A) Process Flow diagram RPB. **(B)** RPB Rotor with flow directions.

Because of these benefits, it is good to have high-quality research on CO_2 capture with RPB absorbers through different experiments and modeling approaches to meet desirable environmental requirements. CO_2 capturing with RPB absorbers is comparatively unexplored and efficient. Thus, it has significant scope for research using different experiments and modeling approaches to meet desirable environmental requirements. Detailed and systematic modeling of RPBs is essential for large-scale CO_2 capture applications because experimental work is a long process and is limited. One can be robust in operation through modeling. Here, RPB models proposed by researchers during the last few years are reviewed and analyzed to predict CO_2 absorption efficiency using different characteristics and modeling approaches.

In this work, the first section reviews the different modeling approaches used in CO_2 capture utilizing RPB. The second contains sub-sections summarizing the study of hydrodynamic characteristics, the study of correlations of mass transfer characteristics of RPB, CO_2 capture modeling and process simulation using RPB, experimental review, and techno-economic analysis. The third section presents a conclusion and proposes fields for future work.

2 Modeling approaches

Various factors such as the rotational speed of RPB, CO_2 partial pressure, liquid-gas flow rate, the temperature of the liquid phase, absorbent concentration, and CO_2 loading solvent affect the

working of an RPB. Numerous modeling techniques based on hydrodynamic analysis and the study of mass transfer characteristics using different operational parameters can be used to examine an RPB. A summary of these techniques is presented in Table 1. The analysis of fluid flow behavior in terms of the liquid holdup, flooding, pressure drop, and liquid flow pattern constitutes the hydrodynamic characteristics. The effect of mass transfer properties of the RPB can be investigated by both gas and liquid phase mass transfer coefficients and effective interfacial area. A numerical approach has been applied to study the process modeling of RPB. Different computational fluid dynamics (CFD) approaches, such as Eulerian-Eulerian or Eulerian-Largrangian, have been used to imitate the gas flow state, fluid drop path, and mass transfer coefficients in an RPB (Zhao et al., 2016). Furthermore, studies have analyzed turbulence models such as k-ε, RNG k-ε, and VOF (Xie et al., 2017; W; Yang et al., 2010; Y; Yang et al., 2015).

Additionally, researchers have also developed machine learning or artificial intelligence to simulate absorption in an RPB using an ANN (artificial neural network). The experimental and modeling approaches can be time-consuming at times. As a result, the ANN approach can be involved. An ANN can be used to predict the coefficient of mass transfer, hydrodynamic parameters, and thermodynamic properties of CO_2 in the absorption process (W. Li et al., 2016; Z. W; Liu et al., 2018; Zhao et al., 2014). Furthermore, expertise in techno-economic analysis is required to grasp the advantage of the proposed project, taking both benefits and costs into account. (T. L. Chen et al., 2020).

2.1 Hydrodynamics parameters

A thorough understanding of hydrodynamic parameters is vital for improving the performance of an RPB system. As a result of the high rotational conditions, the hydrodynamics of the RPBs are altered in ways that significantly affect the gas-liquid mass transfer coefficient. The effect occurs by changing the RPB's hydrodynamics, flooding, liquid holdup, pressure drop, and fluid dispersion.

2.1.1 Liquid holdup (ε_l)

Liquid holdup describes the percentage of liquid volume in the bed after draining. Different correlations have been considered in the literature through modeling depending on the packing type used and flow theory (either film flow or droplet flow). The correlations were then validated with experimental data. These correlations deviate from the existing correlations for conventional columns because of the rotational flow in the RPB.

Basic and Dudukovic (Basic and Dudukovic, n.d.), working under the premise of film flow with complete wetting, presented a correlation for the liquid holdup. It was based on experimental data measured with the electrical resistance measurement method. The research discovered that this expression corresponds with the holdup data as a function of the operational parameters. Furthermore, (Burns et al., 2000) studied the ε_l correlation using the same electrical resistance measurement method with the packing of high porosity. They found that the local packing radius inversely affects the holdup. A practical approach for determining the liquid holdup in RPBs was developed by Y. H. Chen et al. (2004) and involved measuring the quantity of liquid that remained in the RPB after it had stopped operating. The correlation considered the gas flow, which previous researchers had not considered. However, its effect was not that strong and it was observed that ε_l was directly proportional to the liquid flow rate. Y. Yang et al. (2015) derived two correlations for ε_l using different packing. The inference made was that viscosity, liquid flow rate, and rotating speed affect ε_l. Correlations of the liquid holdup are listed in Table 2 for the RPB.

2.1.2 Pressure-drop (ΔP)

Pressure drop indicates the resistance a fluid encounters due to friction or other forces acting on it, such as gravity, and changes with the type of packing. Studies have been made on the empirical correlations of pressure drop with different radii, porosity,

TABLE 1 Modeling approaches for RPB.

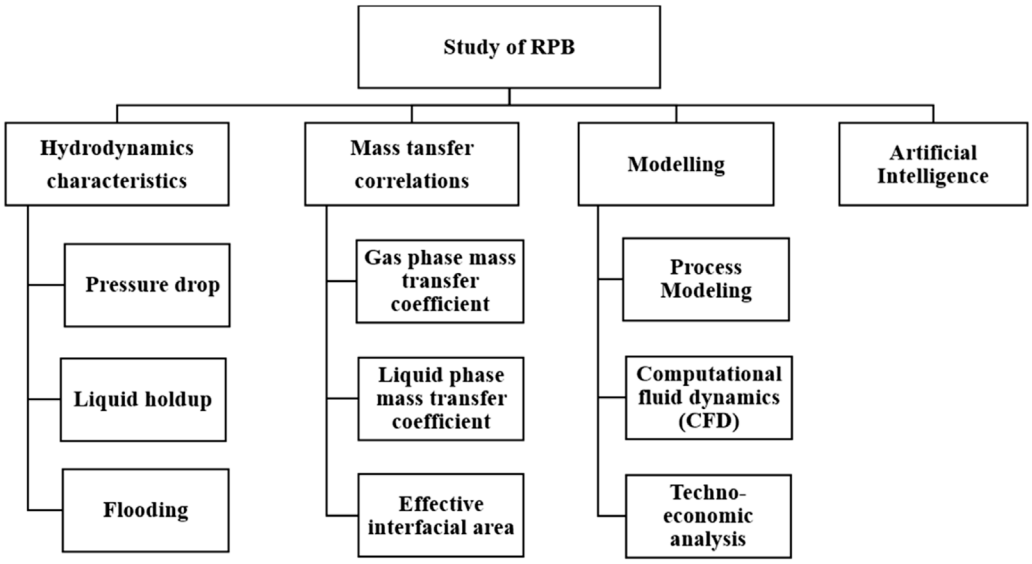

TABLE 2 Liquid holdup correlations for RPB.

Reference	Correlation for ε_l	Material used
Burns et al. (2000)	$\varepsilon_l = 0.039\left(\frac{g}{g_0}\right)^{-0.5}\left(\frac{U_l}{U_0}\right)^{0.6}\left(\frac{\nu}{\nu_0}\right)^{0.22}$	Used reticulated foam with $\varepsilon = 0.953$ *and* $a_s = 786\,m^{-1}$
Chen et al. (2004)	$\varepsilon_l = 21.3\,U_l{}^{0.646}U_g{}^{-0.015}\omega^{-0.148}$	Used stainless steel wire mesh with $\varepsilon = 0.954$–0.956 and $a_s = 793$–$840\ m^{-1}$
Yang et al. (2015)	$\varepsilon_l = 12.159\left(\frac{U_l\rho_l}{a_p\mu_l}\right)^{0.923}\left(\frac{gd_p{}^3}{\nu^2}\right)^{-0.610}\left(\frac{g\mu^4}{\sigma^3\rho}\right)^{-0.019}$	Used wire mesh with $\varepsilon = 0.95$ and $a_s = 497\,m^{-1}$
	$\varepsilon_l = 12.159\left(\frac{U_l\rho_l}{a_p\mu_l}\right)^{0.479}\left(\frac{gd_p{}^3}{\nu^2}\right)^{-0.392}\left(\frac{g\mu^4}{\sigma^3\rho}\right)^{-0.033}$	Used nickel foam with $\varepsilon = 0.8$ and $a_s = 1098\,m^{-1}$
Lu et al. (2019)	$\varepsilon_l = 0.0188\left(\frac{g}{g_0}\right)^{-0.4764}\left(\frac{U_l}{U_0}\right)^{0.5716}\left(\frac{\nu}{\nu_0}\right)^{-0.3197}\left(\frac{\gamma}{\gamma_0}\right)^{-0.7557}$	Used stainless steel wire mesh with $\varepsilon = 0.83$ and $a_s = 1428\,m^{-1}$

interfacial area, and type of packing. Correlations have been developed using these parameters. Keyvani (Keyvani and Gardner, n.d.) used a momentum integral balance on the rotor and the area between the rotor and container to simulate pressure drop. It was observed that ΔP rose with the rise to the square of rotating speed and when gas and liquid flow rates increased. Kelleher Kelleher and Fair, (1996) obtained a correlation between pressure drop and noted that a_c and "Re" is the major contributor to the model. Sandilya et al. (2001) calculated the friction factor of an RPB by investigating the pressure drop. They studied it in two halves, ΔP_0 *and*ΔP_a, using wire gauze. The impacts of gas and liquid flow rates and rotating speed on pressure drop were explored. Chandra et al. (2005) investigated the total pressure drop across the rotor as the sum of pressure drops due to the momentum (ΔP_m), the friction provided by packing (ΔP_f), and the centrifugal force (ΔP_c). It was discovered that the total pressure drop was the sum of ΔP_f; ΔP_c, as ΔP_m was negligible. They also concluded that ΔP across the rotor was directly proportional to gas velocity and rotational speed. The correlations for a given RPB with distinct packing material are given in Table 3.

Here, correlations are derived for a specific RPB with different structures and packing materials. The efficacy of the models or correlations to investigate pressure drops in various RPBs is still to be validated.

2.1.3 Flooding

Flooding occurs when the liquid stops flowing down the column due to the relative vapor flow rates being such that the drag force is higher than or equal to the gravitational force. The flooding phenomenon is different for an RPB compared to conventional columns due to differences in flow area and centrifugal acceleration (Rao et al., 2004). Due to the increased artificial gravity, RPBs may reach larger flooding capacities than conventional columns (Hendry et al., 2020). Two correlations have been used to study flooding: Sherwood's correlation for the packed column and Lockett's correlation for RPB.

Sherwood's approach (Sherwood et al., 1938): $\frac{a_t u_G^2}{ge^3}\left(\frac{\rho_g}{\rho_l}\right)^{0.2}\mu_l^{0.2}$ vs. $\frac{L}{G}\left(\frac{\rho_g}{\rho_l}\right)^{0.5}$ and this gives the flooding limitation.

Wallis's approach (Wallis, 1969) included some more parameters and proposed a relation:

$$C_G^{0.5} + mC_L^{0.5} = C\ where$$

$$C_G = \frac{M_G}{\rho_G A}\left(\frac{\rho_G}{\rho_L - \rho_G}\right)^{0.5}$$

$$C_L = \frac{M_L}{\rho_L A}\left(\frac{\rho_L}{\rho_L - \rho_G}\right)^{0.5}$$

Lockett's approach (Lockett, 1995) for an RPB has the form: $C_G^{0.5} + mC_L^{0.5} = 1.57\beta^{0.25}a_t^{-0.25}\frac{\mu_L}{\mu_w}^{-0.03}$

2.2 Mass transfer correlations

Mass transfer is defined as mass movement from one phase to another. The main reason behind using an RPB instead of the conventional column is its improved mass transfer efficiency. The mass transfer depends on the motion of fluid and hydrodynamic characteristics. Mass transfer of species changes with reaction, time, and space; hence, different mass transfer correlations are used to predict the mass flux of the process. Mathematical modeling of the RPB system requires studying the system of equations based on energy and mass balance, which uses a mass transfer coefficient in the gas-liquid phase and an effective interfacial area. Penetration theory, surface renewal theory, and two film theory are the three theories used to model mass transfer. Based on these theories, different empirical correlations are studied in the literature.

2.2.1 Gas phase mass transfer coefficient (k_G)

Y. S. Chen, (2011) developed a correlation utilizing the two-film theory. The bulk of the data could be accurately predicted using this correlation. The impacts of the flow rates of gas and liquid, the viscosity of the liquid, and centrifugal acceleration on k_G were studied. Furthermore, a comparison of the k_G of the conventional column and the rotating packed bed was made. The k_G was found to be similar in both reactors because the behavior of the gas flow within the rotor was similar to the conventional column. Y. Li et al. (2017) utilized the volumetric gas-side mass-transfer coefficient ($k_G a$) to estimate the local gas phase mass transfer coefficient. This was calculated by air-stripping the ethyl alcohol from an alcohol-water mixture in RZB. They found that the values of k_G was proportional to R_s, gas volumetric flow rate, and liquid volumetric flow rate, according to the experimental data. Research by Lin and Kuo, (2016) showed that mass transfer was achieved in the absorption of CO_2 using a solution of MEA with blade packings in the RPB. They observed that each RPB's k_G value was favorably impacted by the speed of rotation. Moreover, the k_G value depends on the bed's radius, and the flow rates of both the liquid and gas were accompanied by an increase in the k_G values for each RPB. The

TABLE 3 Pressure drop correlations for RPB

Reference	Correlation for ΔP	Material used
Kelleher and Fair (1996)	$\Delta P = \frac{\rho_g \omega^2}{2}(r_0{}^2 - r_i{}^2) + \frac{5B}{22}(\frac{\varepsilon F_G}{\rho_G \pi h})(\frac{1}{r_i{}^{1.1}} - \frac{1}{r_0{}^{1.1}})$	Packing: metal spongelike (85% Nickel and 15% Chromium), $\varepsilon = 0.92$ *and* $a_s = 2500\,m^{-1}, r_0 = 30cm, r_i = 8.75\,cm, h = 15\,cm$
Sandilya et al. (2001)	$\Delta P = \Delta P_a + \Delta P_0$; where $\Delta P_a = \Delta P_c + \Delta P_f + \Delta P_m$; $\Delta P_0 = \frac{1}{2}\rho_g K U_{g,i}^2 + \frac{1}{2}\rho_g (U_{g,0}^2 - U_{g,i}^2)$; $\Delta P_m = \frac{1}{2}\rho_g (\frac{Q_g}{2\pi a e})^2 (\frac{1}{r_i{}^2} - \frac{1}{r_0{}^2})$; $\Delta P_c = \frac{1}{2\varepsilon^2 d_h}\rho_g (\frac{Q_g}{2\pi a})^2 [\alpha \frac{2\pi a \nu_g}{Q_g d_p} ln \frac{r_0}{r_i} + \phi\beta(\frac{1}{r_i{}^2} - \frac{1}{r_0{}^2})$; $\Delta P_f = \frac{\lambda}{2\varepsilon^2 d_h}\rho_g (\frac{Q_g}{2\pi a})^2 [\alpha \frac{2\pi a \nu_g}{Q_g d_p} ln \frac{r_0}{r_i} (\sum_{j=1}^{n} ln \frac{r_{0j}}{r_{ij}}) + \beta \sum_{j=1}^{n} (\frac{1}{r_{ij}{}^2} - \frac{1}{r_{0j}{}^2})]$	Packing: wire mesh, $\varepsilon = 0.91$ *and* $a_s = 2196\,m^{-1}, r_0 = 0.155\,m, r_i = 0.155\,m, h = 0.022\,m$
Chandra et al. (2005)	$\Delta P = \Delta P_c + \Delta P_f + \Delta P_m$	Packing: split ring, for rotor 1: $\varepsilon = 0.8$ *and* $a_s = 1180\,m^{-1}, h = 0.028\,m$ for rotor 2: $\varepsilon = 0.9$ *and* $a_s = 1780\,m^{-1}, h = 0.03\,m$
Lin and Jian (2007)	$\Delta P = \frac{F_r^2}{2}\frac{a_s}{(\varepsilon - \varepsilon_l)^3} f_w (r_o - r_i)$	Packing: wire mesh, $\varepsilon = 0.97$ *and* $a_s = 299\,m^{-1}, r_0 = 0.0625\,m, r_i = 0.0195m, h = 0.0295m$

TABLE 4 Gas phase mass transfer coefficient correlation in RPB.

Reference	Correlation for k_G	Material used
Onda et al. (1968)	$\frac{k_G RT}{a_t D_G} = 5.23(\frac{G}{a_t \mu_G})^{0.7}(\frac{\mu_G}{\rho_G D_G})^{\frac{1}{3}}(a_t D_p)^{-2}$	Studied in the system of CO_2 with NaOH in packed column and for RPB' g' is replaced by 'r ω^2'
Liu et al. (2016)	$k_G a_e = 0.01043 Re_G{}^{1.0738} We_L{}^{0.1192} Ga^{0.09007}$; $k_G a_e = 0.01081 Re_G{}^{1.0281} We_L{}^{0.090841} Ga^{0.09081}$	Investigated using structured nickel foam packing in the system of SO_2-NaOH
Su et al. (2018)	$\frac{k_G a_e d_p}{a_t D_G} = 0.456 Re_L{}^{0.59} Re_G{}^{0.63} We_L{}^{0.07} Fr_L{}^{-0.06}(\frac{\sigma}{\sigma_c})^{0.10}$	Studied in counter airflow shear RPB using the system NH_3-H_2O
Chen (2011)	$\frac{k_G a_e d_p}{a_t{}^2 D_G}(1 - 0.9\frac{V_o}{V_t}) = 0.023 Re_L{}^{0.14} Re_G{}^{1.13} We_L{}^{0.07} Gr_G{}^{0.31}(\frac{a_t}{a_p})^{1.4}$	Studied absorption and stripping in RPB of ammonia and volatile organic compounds

correlations for k_G found in the literature have been presented in Table 4.

2.2.2 Liquid phase mass transfer coefficient (k_L)

Absorption usually occurs in liquid, hence the k_L model must be validated using experimental data to explain system behavior. Mass transfers are generally determined in RPBs using $k_L a$ instead of k_L to overcome the difficulties in predicting the interfacial area, a_e. With the use of penetration theory, Tung and Mah (Tung and Mah, 1985) replaced gravitational acceleration with centrifugal acceleration to develop a correlation in an RPB for the k_L. This study did not use the effect of Coriolis acceleration and the geometry of the material used in packing. (Luo et al., 2012a) computed $k_L a$ using surface renewal theory. They found a margin of error between the experimental results and the model predictions of nearly 15%. This was based on the premise that liquid droplets were present in blade packing. Y. S. Chen et al. (2005) examined the mass transfer effectiveness in an RPB with distinct packed bed radii and considered end effects for the calculation of $k_L a$ in an RPB. This was applied to RPBs of various diameters and viscous Newtonian and non-Newtonian fluid systems. Similar correlations have been studied in the literature and are shown in Table 5.

2.2.3 Effective interfacial surface area

Effective interfacial surface area (a_e) is used to define the mass transfer properties of a reactor and is mostly affected by hydrodynamic properties. Correlations on the a_e in conventional columns, studied by Onda et al. (1968); Billet and Schultes, (1999), have been used for RPBs by replacing "g" with "r ω^2". Tsai and Chen, (2015) studied this correlation and noticed that the effective interfacial surface area was influenced by the speed of the rotor and F_l . Chu et al. (2015) looked at the effective interfacial area using nickel foam packing and a combination of static rings and rotational packing. A rotor of two-stage counter-current RPB was used. The efficiency of CO_2 absorbed and a_e were evaluated using cutting-edge "five-point" techniques. Experiments showed that the lower and upper packing zones were much better at absorbing CO_2 than the upper and lower cavity zones. This was true for distinct R_s and liquid-gas flow rates. The correlations studied in the literature are tabulated here in Table 6.

The correlation of k_G, k_L, and a_e are highly influenced by the experimental data and the fitting function used. As a result, generalizing the found correlations to other RPBs or operating situations is problematic.

2.3 Process modeling review

Process modeling is a technique used to predict the behavior of a system through computer techniques and graphical representation. It is further used to understand the influence of parameters on the system. Developing an RPB model involves chemical reaction equations, rate constants, and relations for calculating physical properties. These equations are included in the process modeling algorithm using tools for simulation and analysis and are shown here through a flowchart in Figure 2. For an RPB, a process model will be helpful

TABLE 5 Liquid phase mass transfer coefficient correlation in RPB.

References	Correlation for k_L	Material used
Tung and Mah (1985)	$\frac{k_L d_p}{D_L} = 0.919 Sc_L^{0.5} Re_L^{1/3} \left(\frac{d^3 \rho^2 g}{\mu^2}\right)^{1/6} \left(\frac{a_t}{a}\right)^{1/3}$	Investigated with the stack of disc like cages mounted on a vertical rotor and replaced g with r ω^2.
Jiao et al. (2010)	$k_L a_e = 0.003689 Re_G^{0.5449} We_L^{0.5476} Ga^{0.3428}$	Designed the correlation in a cross flow RPB with a solution system of CO_2-NaOH with a packing of porous plate
Chen et al. (2006)	$\frac{k_L a_e d_p}{a_t D_L}\left(1 - 0.93\frac{V_o}{V_t} - 1.13\frac{V_i}{V_t}\right) = 0.35 Sc_L^{0.5} Re_L^{0.17} We_L^{0.3} Gr_L^{0.3} \left(\frac{a_t}{a_p}\right)^{-0.5} \left(\frac{\sigma_C}{\sigma_w}\right)^{0.14}$	Different types of packing surfaces such as stainless beads and acrylic beads, and raschig rings wire mesh and intalox saddles were used for the study in the system of oxygen with water
Zhang et al. (2011)	$\frac{k_L a_e d_p}{a_t D_L} = 8.813 Sc_L^{0.5} We_L^{0.335} Gr_L^{0.37}$	Correlation investigated using ionic liquids for CO_2 capture

TABLE 6 Effective interfacial surface area.

Reference	Correlation for a_e	Material used
Onda et al. (1968)	$\frac{a_e}{a_t} = 1 - \exp\left[-1.45 Re_L^{0.1} Fr_L^{-0.05} We_L^{0.2} \left(\frac{\sigma_c}{\sigma_L}\right)^{0.75}\right.$	Absorption of CO_2 in a packed column
Rajan et al. (2011)	$\frac{a_e}{a_t} = 11906 Re_L^{-1.8070} Fr_L^{-0.0601} We_L^{0.9896}$	Studied in split packing of Ni-Cr metal foam with chemisorption of CO_2-NaOH
Luo et al. (2012b)	$\frac{a_e}{a_t} = 66510 Re_L^{-1.41} Fr_L^{-0.12} We_L^{1.21} \left(\frac{c^2}{(c+d)^2}\right)^{-0.74}$	Used CO_2-NaOH absorption for the investigation with structured stainless steel wire mesh packing
Luo et al. (2017)	$\frac{a_{ep}}{a_t} = 15.17 Re_G^{0.16} Re_L^{-0.38} Fr_L^{-0.13} Wr_L^{0.45} \left(\frac{c^2}{(c+d)^2}\right)^{-0.29}$	Used CO_2-NaOH absorption for the investigation with structured stainless steel wire mesh packing

for design, scaling up, debugging, process monitoring, mechanistic understanding, and optimal design and process evaluation. RPB modeling studied by various researchers is reviewed in this section.

The assumptions made for the model and the calculation of the operational properties are different in different modeling studies. Since the shape of an RPB is circular, the common assumptions made by the researchers are that the flow of fluids is in counter-current and radial directions, shown in Figures 1A, B. To simulate the RPB, distinct theories have been proposed for mass transfer, such as penetration theory, film theory, and surface renewal theory. Sun et al. (2009) established a mathematical system for the absorption of CO_2 and NH_3 in water for an RPB. The mass equation of CO_2 in a droplet, as well as the film zone, was expressed in terms of a partial differential equation with Neumann boundary conditions. Through the model, an overall volumetric mass transfer coefficient ($K_G a$) was predicted. Furthermore, it was observed that $K_G a$ was proportional to rotational speed, the volumetric flow rate of gas and liquid, and the NH_3/H_2O mole ratio. Kang et al. (2014) suggested an absorption model of CO_2, using MEA with the mass transfer, that uses two film theory. A system of differential equations based on material and energy balance equations has been developed for the gas and liquid phases. The boundary conditions were taken on the concentration of components and temperature of the gas and liquid phases at the inner-outer radii of the RPB. The proposed model took into account water evaporation and did not rely on the isothermal assumption. Joel et al. (2015) studied the rate-based model to analyze mass transfer using two sets of correlations in an RPB. The model has been implemented in FORTRAN and linked to ASPEN Plus. Through model validation, it was discovered that the second set

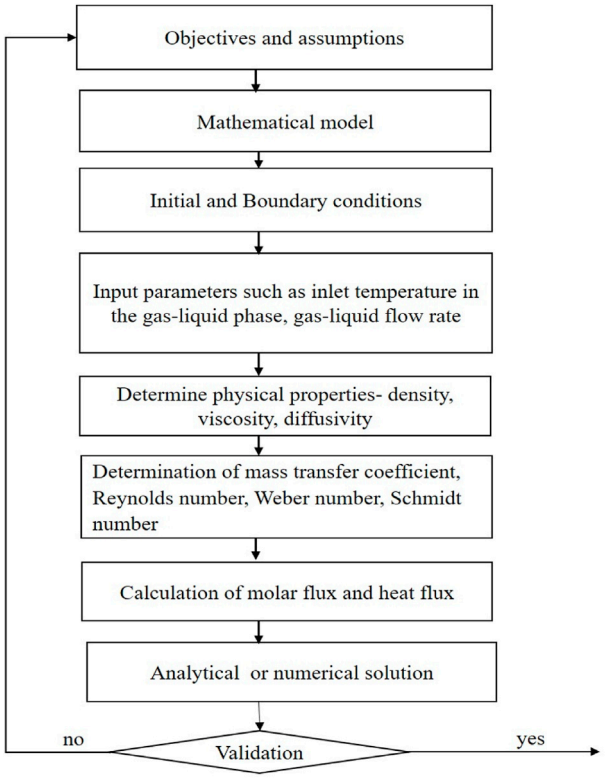

FIGURE 2
Flowchart for the modeling procedure of RPB.

TABLE 7 Modeling of RPB for CO_2 capture.

No.	Solvent	Mathematical equations	Methodology	Validation
1	MDEA	$k_g a_t\,(y_{CO_2} - \frac{H}{P}\frac{1}{K_2K_3}\frac{(c_{R_3N,total}-c_{R_3N})c_{HCO_3^-}}{C_{R_3N}})2\pi hrdr = G_{N_2}\mathrm{d}(\frac{y_{CO_2}}{1-y_{CO_2}})$ $k_L a_t \frac{P}{H}\,(y_{CO_2} - \frac{H}{P}\frac{1}{K_2K_3}\frac{(c_{R_3N,total}-c_{R_3N})c_{HCO_3^-}}{C_{R_3N}})2\pi hrdr = F_l d(c_{HCO_3^-})$ $-k_L a_t \frac{P}{H}\,(y_{CO_2} - \frac{H}{P}\frac{1}{K_2K_3}\frac{(c_{R_3N,total}-c_{R_3N})c_{HCO_3^-}}{C_{R_3N}})2\,\pi hrdr = F_l d(c_{R_3N})$	Model uses penetration theory for studying mass transfer and built differential mass balance for CO_2 and differential mole balance for HCO_3- and R_3N in both phases. The BVP was converted to IVP and solved using Runge Kutta Fehlberg (RKF45) programmed in FORTRAN.	Qian et al. (2009)
			Observation	Reference
			The solution describes the absorption of CO_2, and the model predicts the mole fraction of CO_2 in outlet gas with a 4% deviation from the experimental data. Also, the effects of rotating speed, liquid flow rate, and temperature on the mass transfer coefficient were analyzed	Qian et al. (2009)
2	DEA-K (.Benfield solution)		Methodology	Validation
		$N_{CO_2}2\pi hrdr = G_{N_2}d(\frac{y}{1-y})$ $-N_{CO_2}2\pi hrdr = d(F_l c_{CO_{3^{2-}}})$ $2N_{CO_2}2\pi hrdr = d(F_l c_{HCO_{3^-}})$	Established a steady-state model on the absorption of CO_2 at higher levels of gravity. The mole balance for CO_2 was expressed as an ordinary differential equation with respect to the radius of RPB and was solved using the algorithm of shooting method in MATLAB.	Yi et al. (2009)
			Observation	Reference
			The mole fraction of CO_2 in outlet gas was predicted and validated with self-experimental data with 10% deviation. Also, the effects of temperature, gas-liquid flow rate, rotational speed, and end effect on the mass transfer efficiency were anticipated using the model	Yi et al. (2009)
3	NaOH-CO_{22}		Methodology	Validation
		$\frac{\partial c_{co_2}}{\partial t} = \frac{D_{CO_2,L}}{r^2}\frac{\partial}{\partial r}(r^2\frac{\partial c_{CO_2}}{\partial r}) + (-k_{r1}c_{CO_2}c_{OH^-})$ $\frac{\partial c_{OH^-}}{\partial t} = \frac{D_{OH^-,L}}{r^2}\frac{\partial}{\partial r}(r^2\frac{\partial c_{OH^-}}{\partial r}) + (-k_{r1}c_{CO_2}c_{OH^-} - k_{r2}c_{Hco_3^-}c_{OH^-})$ $\frac{\partial c_{Hco_3^-}}{\partial t} = \frac{D_{Hco_3^-,L}}{r^2}\frac{\partial}{\partial r}(r^2\frac{\partial c_{CO_2}}{\partial r}) + k_{r1}c_{CO_2}c_{OH^-} - k_{r2}c_{Hco_3^-}c_{OH^-}$ $\frac{\partial c_{co_3^{2-}}}{\partial t} = \frac{D_{co_3^{2-},L}}{r^2}\frac{\partial}{\partial r}(r^2\frac{\partial c_{co_3^{2-}}}{\partial r}) + (k_{r2}c_{Hco_3^-}c_{OH^-})$	The mathematical model of mass transfer characteristics was presented using the partial differential equation in spherical coordinates, and method on line (MOL) was used employed in MATLAB using pdepe and pdeval inbuilt function. In addition, the influence of the Higee factor, gas and liquid flow rate, pressure, temperature, and other parameters on CO_2 absorption mass transfer characteristics was studied	Gao et al. (2016)

(Continued on following page)

TABLE 7 (*Continued*) Modeling of RPB for CO_2 capture.

No.	Solvent	Mathematical equations	Methodology	Validation
			Observation	Reference
			CO_2 concentration distribution in a droplet was estimated, further k_L was calculated and employed for the determination of the mass transfer rate per volume. An increase in temperature and liquid flow rate and pressure has been found to boost the efficiency of CO_2, while an increase in gas flow rate has the opposite effect. The created model describes the diffusion-reaction mass transfer mechanism of CO_2 absorption in an RPB with a deviation of ± 20%	Gao et al. (2016)
4	MEA		Methodology	Validation
		$\frac{\partial(y_i F_g)}{\partial r} = a_{gl} N_i A_c$ $\frac{\partial(x_i F_l)}{\partial r} = a_{gl} N_i A_c$ $\frac{\partial(T_g C_{pg} F_g)}{\partial r} = a_{gl} q_g A_c$ $\frac{\partial(T_l C_{pl} F_l)}{\partial r} = a_{gl} q_l A_c$	The two-film theory was used to compute the mass transfer flux in a steady-state model. The differential equation system was framed using mass and energy balance equation in the gas-liquid phase, and the 2nd order finite difference method-based SRADAU solver was used in gPROMS to solve it. Based on this, the impact of five enhancement factors and eight alternative kinetic reaction models was explored	(S Jassim, 2002)
			Observation	Reference
			It was observed that the kinetic model has an effect on CO_2 capture while the enhancement factor has no much effect. With the help of the model, process analysis was also made and validated with experimental data with a 3.5% deviation	Borhani et al. (2018)
5	MEA		Methodology	Validation
		$\varepsilon_g \frac{\partial C_{g,i}}{\partial t} = \frac{-1}{2\pi r h} \frac{\partial(y_i F_g)}{\partial r} - a_{gl} N_i$ $\varepsilon_l \frac{\partial C_{l,i}}{\partial t} = \frac{1}{2\pi r h} \frac{\partial(x_i F_l)}{\partial r} - a_{gl} N_i$ $\varepsilon_g C_g C_{v,g} \frac{\partial T_g}{\partial t} = \frac{-C_{pg} F_g}{2\pi r h} \frac{\partial(T_g)}{\partial r} + a_{gl} h_{gl} (T_l - T_g)$ $\varepsilon_l C_l C_{p,l} \frac{\partial T_l}{\partial t} = \frac{-C_{pl} F_l}{2\pi r h} \frac{\partial(T_l)}{\partial r} + a_{gl} (h_{gl} (T_l - T_g) - \Delta H_{rxn} N_{CO_2} - \Delta H_{vap,H2O} N_{H2O} - \Delta H_{vap,MEA} N_{MEA}$	A steady-state model is presented of RPB absorber and stripper and uses a gPROMS solver. For the solution in the gas phase forward difference method is used, while in the liquid phase backward finite difference method is used which is based on flow directions. Also, an optimization solution was obtained for the energy minimization, which was also solved in gPROMS using NLPSQP solver	Cheng et al. (2013), S Jassim (2002)
			Observation	Reference
			An investigation was conducted to review the effect of the decision variables on the optimization	Im et al. (2020)

(Continued on following page)

TABLE 7 (*Continued*) Modeling of RPB for CO_2 capture.

No.	Solvent	Mathematical equations	Methodology	Validation
6	PZ + MDEA		Methodology	Validation
		$\frac{\partial(y_i F_g)}{\partial r}\frac{1}{2\pi r h} = a\,N_i\,\varepsilon$ $\frac{\partial(x_i F_l)}{\partial r}\frac{1}{2\pi r h} = a\,N_i\,\varepsilon$ $\frac{\partial(T_g C_{pg} F_g)}{\partial r}\frac{1}{2\pi r h} = a\,q_G\,\varepsilon$ $\frac{\partial(T_l C_{pl} F_l)}{\partial r}\frac{1}{2\pi r h} = a\,q_l\,\varepsilon$	A model was prepared using MATLAB linked with ASPEN to predict the CO_2 removal using a blended amine solution. The equations were written in MATLAB, and physical properties were obtained from ASPEN. The impact of five different parameters on CO_2 absorption efficiency has been studied and validated with experiments	Zhan et al. (2020)
			Observation	Reference
			This model was helpful in predicting the CO_2 absorption efficiency, overall mass transfer coefficient, CO_2 loading, and CO_2 concentration in the gas medium and validated with experimental data with less than a 7% deviation	Esmaeili et al. (2022)

of correlations was superior. Furthermore, it was determined that the amount of CO_2 captured and the flue gas flow rate rises with an increase in lean-MEA temperature. The model validation reports for the RPB, along with the modeling and simulation for CO_2 capture, are presented in Table 7.

The reliability of these models is significantly dependent on the availability and effectiveness of existing correlations. As a result, developing trustworthy correlations is the foundation for adequately simulating the process using different modeling software. Various correlations with regard to mass transfer are tabulated in Tables 4, 5. The relation shows the internal connection of distinct operational parameters, physical properties of the process, and dimensionless numbers using the different packing materials. Other researchers studied the correlations of k_G, k_L, and a_e Taking different operational parameters, regressing constants' values, and validating the relations with experimental data. These characteristics can also be interpreted and simulated using CFD as it can analyze the flow behavior in a better way. Hence, good predictions of these characteristics could be achieved.

2.4 Review of experimental data with RPB

In recent years, for the reduction of CO_2 emissions, a PCC process with the RPB technique has been investigated. Many researchers are working to determine CO_2 absorption efficiency in an RPB with different packing materials, dimensions of the equipment, and operational parameters. An experiment on the chemical absorption of CO_2 was conducted by Cheng and Tan, (2009) in an RPB utilizing a combination of amine solvents (MEA, AEEA, PZ, and AMP). The researchers found that higher temperatures increased absorption efficiency (303–333 K). It was also shown that a higher percentage of PZ in the mixture results in higher capture efficiency. For CO_2 absorption, Mohammadi Nouroddinvand and Heidari, (2021) performed experimental results employing an Arc-blade RPB in MEA (0.5–2.0 M) solvent. Wire mesh in the stainless-steel packaging was used. Two rectangular gas inlets, each 75 mm in length and 3 mm wide, were employed instead of circular designs. The obtained efficiency for capturing CO2 was 49%–78%, with $F_G = 56\frac{l}{min}, F_l = 0.3 - 0.6\,l/min$,; $R_S = 300 - 1200\,rpm$. Utilizing the tri-solvent of N-methylpyrolidone (NMP), amorphous ammonium phosphate (AMP), and AEEA (2-(2-aminoethylamino) ethanol), Y. Wang et al. (2021) studied the absorption and desorption process for CO_2 capture in RPB. The measured CO_2 absorption efficiency was 89%. The findings reveal that this approach has promising industrial applicability, with a regeneration consumption of energy of 2.46 GJ/ton CO_2. Single and blended amines MEA, 2-methylamino-ethanol (MME), and PZ ranging from 30 to 100 wt% were tested for their ability to capture CO_2 in an RPB by Ma and Chen (Ma and Chen, 2016). The experimental findings revealed that the CO_2 removal efficiency was greatly enhanced by raising the alkanolamine concentration and the R_S up to 1800 rpm. However, when the F_g rose, the removal efficiency declined. Since MMEA interacts with CO_2 at a quicker rate than MEA, MMEA-based systems demonstrated greater efficiency in the removal process. Mixtures of alkanolamines with PZ were more efficient at sequestering CO_2 than either component used alone. Table 8 presents the summary of the experimental data from the literature, which gives a comparison of different performance studies using an RPB and would help in deciding on experimental conditions for future experiments.

2.5 Techno-economic analysis

Implementing an RPB helps lower operating costs and environmental impact by reducing reactor size and capital expense. There are few studies in the literature that compare

TABLE 8 Experimental data review.

Reference	Solvent and dimension of RPB	Operating conditions	Objective	Results
Mohammadi Nouroddinvand and Heidari (2021)	Solvent: MEA Radius of Arc RPB = 0.155 m; $r_0 = 0.14m$; $r_i = 0.04m$; h = 0.098 m; Vol. of packing = 0.005542 m^3; $\varepsilon = 0.9882$	$R_s = 300 - 1200\,rpm$; CO_2 inlet concentration = 5,000–20000 ppm; MEA solution = 0.5M–2M; $F_l = 0.3 - 0.6\,l.min^{-1}$; $F_g = 56\,l.min^{-1}$	Arc-blade RPB, a new design introduced	With increase in R_s,CO_2 absorption enhanced to 9%
			Effect of solvent concentration, R_s, gas-liquid inlet flow ratio on absorption efficiency in new RPB was studied	With CO_2 inlet concentration and MEA concentration from 0.5 to 1M, absorption efficiency enhanced by 10% in Arc-blade RPB
Ma and Chen (2016)	Solvent: MEA, MMEA, PZ $r_0 = 6cm$; $r_i = 2.25cm$; h = 1.8 cm; surface area of packing = 1,229 m^2/m^3; $\varepsilon = 0.93$	$R_s = 600 - 2400\,rpm$; T = 313 K CO_2 inlet concentration = 10 vol %; $F_l = 0.1\,l.min^{-1}$; $F_g = 30 - 70\,l.min^{-1}$	Concept of blended amine using tri-solvent was introduced	CO_2 removal efficiency rose with rise in R_s and decline in F_g
			Effect of R_s, F_g and composition of the absorbent were studied	MMEA shows good removal efficacy. 99.4% CO_2 removal efficiency with HTU = 0.74 was obtained
Wang et al. (2021)	Solvent: AMP, AEEA, NMP $r_0 = 9.5cm$; $r_i = 2.25cm$; h = 2.3 cm; surface area of packing = 500 m^2/m^3; $\varepsilon = 0.95$	$R_s = 600 - 1400\,rpm$; T = 298.15–333.15 K CO_2 inlet concentration = 14%; $G/L\,Ratio = 100 - 260\,l/l$; Pressure = 1 bar Residence time = 0.69–2.08 sec	Study was conducted to know the feasibility of using tri-solvent for CO_2 capture	For absorption, CO_2 capture efficiency is 89% and K_G = 2.67 kmol/m^3 hr.kPa for loading = 0.035 mol CO_2/mol amine
			DSS technique is used for desorption for solving the challenge of steam scarcity while stripping	DSS technique reduced energy consumption which is 36.6% lower than conventional reboiler
Cheng and Tan (2009)	Solvent: MEA,AMP, AEEA, PZ $r_0 = 8cm$; $r_i = 3.8cm$; h = 2 cm	$R_s = 400 - 1600\,rpm$; CO_2 inlet concentration = 10 vol% T = 303–333 K $F_l = 100 - 300\,ml.min^{-1}$; $F_g = 3 = 20 - 70\,l.min^{-1}$	CO_2 capture was studied for 10 vol% of CO_2 and 30wt% of mixed amine by chemical absorption	CO_2 capture depends on R_s, F_g, F_l and increase with temperature
			Effect of R_s, F_g, F_l, and temperature was studied	For CO_2 loading, regeneration energy, and lower HTU, a combination of 15 wt% PZ and 15% MEA or AEEA was observed to be effective
Chamchan et al. (2017)	Solvent: MEA $r_0 = 0.18m$; $r_i = 0.06m$; h = 0.06 m; vol. of packing = 5,428 m^3; $\varepsilon = 0.9832$	$R_s = 1600\,rpm$; $F_l = 110 - 130\,kg.hr^{-1}$; $inlet\ F_g = 241.11 - 285.37\,mol.hr^{-1}$ $outlet\ F_g = 176.07 - 204.99\,mol.hr^{-1}$	Comparison made between Packed bed (PB) and RPB with PB stripper in a pilot plant with 30 wt% MEA	Both packed bed (PB) and RPB show the same amount of energy consumption with a one-third reduction in the volume of RPB to PB.
Kang et al. (2014)	Solvent: dilute aqueous ammonia $r_0 = 6.25cm$; $r_i = 1.25cm$; h = 2.3 cm; surface area of packing = 887.6 m^2/m^3; $\varepsilon = 0.96$	$R_s = 400 - 1600\,rpm$; T = 300 K CO_2 inlet concentration = 30%; $F_l = 0.05 - 0.25\,l.m^{-1}$; $F_g = 10 - 25\,l.m^{-1}$; p = 1 atm	Experimental data studied for PB and RPB using dilute aqueous ammonia for CO_2 absorption	HTU = 0.08–0.40 m for RPB and HTU = 0.35–1.96 m for PB. HTU of RPB was smaller than PB

(Continued on following page)

10.3389/fenrg.2023.1135188

TABLE 8 (*Continued*) Experimental data review.

Reference	Solvent and dimension of RPB	Operating conditions	Objective	Results
Jassim et al. (2007)	Solvent: MEA $r_0 = 19.9cm$; $r_i = 7.8cm$; h = 2.5 cm; vol. of packing = 0.883 m^3; $\varepsilon = 0.76$	$R_s = 600 - 1000\,rpm$; T = 293–313 K CO_2 inlet concentration = 10 vol %; Overall gas flow rate = $p = 1$ atm	Measurement of CO_2 absorption and desorption with 30 wt% MEA.	Results were obtained using 30, 55, 75, and 100 wt% MEA for CO_2 absorption
			Effect of amine temperature, peripheral rotor gravity (31 and 87 g), and MEA concentration were investigated	Comparison of PB and RPB absorber was made. Comparison with stripper was also made and observed that RPB has advantage of size reduction over PB at similar operational conditions

the environmental and economic effects of the RPB process to a conventional column process. There are benefits of using an RPB over the conventional column. Joel et al. (2014) compared conventional columns and RPBs and found that reduction in size had a crucial influence on absorption efficiency. Cheng et al. (2013) investigated the regenerator's regeneration energy and found that an RPB with just a 10th of the volume of a conventional column could achieve the same regeneration efficiency. As a result of the enhanced heat transfer zone in the RPB, less vapor lean MEA needed to be transferred from the reboiler to the RPB. R. Zhang et al. (2017) used three mixed solvents MEA-MDEA-PZ, to study CO_2 absorption and desorption. An increase in the MDEA/PZ mole fraction among these blends resulted in a reduction in energy use and an increase in the rate of CO2 absorption. They also looked at the MEA-MDEA-PZ combination, which compared to 5M MEA, used 15.22%–49.92% less energy. M. Wang et al. (2015) noted that an RPB has good mass transport properties and is the most suited-technique for PCC. The performance of an RPB was methodically assessed from the engineering, environmental, economic, and energy perspectives by T. L. Chen et al. (2020). To propose a superior technical option compared to current CCSU facilities, a cost-benefit analysis was carried out utilizing running costs, carbon credit, and reductions in air quality. According to (Otitoju et al., 2023), packed bed absorbers' and strippers' size adds to the problems. If the absorbers and strippers can be replaced with RPB equivalents, CO_2 collection could be better and cheaper. A rate-based model in the steady state of the RPB absorber was proposed and verified for this study using Aspen Custom Modeller. It was used to perform technical and economic evaluations of operating big RPB absorbers using concentrated MEA (55–75 wt%). Compared to packed bed absorbers, the RPB absorber reduced the volume by a factor of 4–11 at a concentration of 55 wt% MEA, according to the technical evaluations, and had lower capital costs while having the largest volume reduction factors (3%–53% lower).

In conclusion, based on thorough and precise process models, it is necessary to estimate the entire costs (capital and operational expenses) utilized to capture CO_2 in intensified and traditional PCC processes. Different modeling approaches have been discussed in detail. The conclusion reached in this context is that the solution of the model for carbon absorption depends on the conservation of mass and energy balance equation with appropriate model assumptions and using appropriate relations for simplifying and solving the system of equations. The CO_2 mole fraction is predicted in outlet gas at numerous liquid flow rates, rotational speeds, and temperatures. The impact of different operating factors on the coefficient of mass transfer in RPB can be anticipated with the aid of a model. In addition to describing how mass transfer intensification occurs in an RPB, the gas-liquid mass transfer characteristic mathematical model also provides a theoretical foundation for the creation of RPBs and their actual application. Techno-economic analysis was discussed, which is necessary to optimize the entire expense utilized in CO_2 capture with an RPB having advantages over the conventional column. In chemical absorption, further research is needed to reduce solvent degradation, reducing the requirement for solvent make-up and, consequently, decreasing operational costs. New configurations and

integration arrangements will contribute to cutting down energy consumption and, ultimately, minimizing expenses. Additives, for example, may be used to decrease surface tension and contact angles and thereby increase absorption rates utilizing CO_2 transfer and solvent wetting. The challenges that remain are actively being pursued across the policy, economic, environmental, and technology communities at all levels.

From the viewpoint of reducing emissions of CO_2 into the atmosphere, carbon capture utilization and sequestration (CCUS) technology needs to be retrofitted into power plants. Research has been done on the modeling and simulation of CO_2 capture for the conventional column, but an RPB is more efficient. More research is required in this domain to make the process of CO_2 capture faster with a lower cost. In the future, more modeling attempts are necessary for RPB absorbers in a steady and dynamic state with different solvents. Better operational parameters which influence the mass transfer of fluids are being investigated, which need to be studied to enhance the predictions of mass flux and CO_2 absorption efficiency. Furthermore, factors that influence the cost of the process need to be investigated for techno-economic analysis so that the process of CO_2 capture also becomes cost-effective. Utilizing CFD and an ANN are also promising approaches for studying hydrodynamic characteristics and mass transfer. The theoretical analysis and modeling of the RPB regenerator is the new scope of research work required. Understanding the complete absorption and desorption process through absorber and desorber together will scale up the CO_2 capture process.

3 Conclusion and future scope

RPB process intensification technology for the PCC process fits under sustainable development and industrial decarbonization. An RPB is a better option for CO_2 capture due to its advantages compared to the conventional column. However, it still has some disadvantages, such as large pressure drops and other mechanical wear and tear issues. The conventional column requires a considerable height, high capital cost, and more energy efficiency to regenerate the solvent. This equally applies to an RPB as it is a regenerative chemical absorption process. Both processes require energy-efficient solvents for cost-effective CO2 capture. Because the factors that affect the CO_2 absorption efficiency depend on hydrodynamic studies, mass transfer correlations, rotating speed, solvent characteristics, and fluid flow rates, this article reviews all these factors. The correlation of hydrodynamic parameters, mass transfer in the gas-liquid phase in RPBs, and process modeling of large-scale RPBs studied in the literature will help to determine the efficiency of CO_2 absorption in any amine-based solvent using RPB technology. A reasonable interpretation of the whole process can thus be made. The centrifugal surroundings have a significant influence on mass transport by modifying the hydrodynamics of an RPB. As a result, a thorough grasp of this is required to improve an RPB's mass transfer performance.

Different hydrodynamic characteristics were discussed. The distinct correlations of liquid holdup and pressure drop in RPBs were summarised and showed that the parameters that affect pressure drop are rotational speed and centrifugal acceleration. Furthermore, studies were made to determine the influence of flow rates on pressure drop. The parameters that affect liquid holdup depend on velocity, rotor speed, and the packing structure. Hence, correlations using these parameters were discussed. The understanding of mass transfer is essential as it has a significant effect on the absorption of CO_2. Experimental studies with MEA and other amines/blended amines were explored. As pilot plant and scale-up studies are essential, this review provides a direction for a future CO_2 capture study in a pilot process with an energy-efficient solvent at the CO2 research center of our university.

Author contributions

CS: Analysis and interpretation; methodology; writing–original draft; review and editing. SD: Conceptualization; resources; project administration, supervision writing—review and editing. PM: Supervision; validation; writing review and editing.

Acknowledgments

The authors are thankful for financial support from the Department of Biotechnology (DBT), Ministry of Science and Technology, Govt. of India; through the project "Integrated Design and Demonstration of Intensified CO_2 Capture with cost-effective advanced Process. (INDIA-CO2)," No. T/PR31120/PBD/26/755/2019.

Conflict of interest

The authors declare that the research was conducted in the absence of any commercial or financial relationships that could be construed as a potential conflict of interest.

Publisher's note

References

Afkhamipour, M., and Mofarahi, M. (2013). Comparison of rate-based and equilibrium-stage models of a packed column for post-combustion CO2 capture using 2-amino-2-methyl-1-propanol (AMP) solution. *Int. J. Greenh. Gas Control* 15, 186–199. doi:10.1016/j.ijggc.2013.02.022

Akanksha, Pant, K. K., and Srivastava, V. K. (2007). Carbon dioxide absorption into monoethanolamine in a continuous film contactor. *Chem. Eng. J.* 133 (1–3), 229–237. doi:10.1016/j.cej.2007.02.001

Ayash, A. A., and Mahmood, M. A. (2022). Conventional and non-conventional gas-liquid contacting methods: A critical review and a quantitative evaluation. *AIP Conf. Proc.* 2660. doi:10.1063/5.0107723

Basic, A., and Dudukovic, M. P. (n.d.). Liquid holdup in rotating packed beds: Examination of the film flow assumption. *AIChE J.* 41 (2), 301–316. doi:10.1002/aic.690410212

Billet, R., and Schultes, M. (1999). Prediction of mass transfer columns with dumped and arranged packings: Updated summary of the calculation method of Billet and Schultes. *Chem. Eng. Res. Des.* 77 (6), 498–504. doi:10.1205/026387699526520

Borhani, T. N., Oko, E., and Wang, M. (2018). Process modelling and analysis of intensified CO2 capture using monoethanolamine (MEA) in rotating packed bed absorber. *J. Clean. Prod.* 204, 1124–1142. doi:10.1016/j.jclepro.2018.09.089

Burns, J. R., Jamil, J. N., and Ramshaw, C. (2000). Process intensification: Operating characteristics of rotating packed beds - determination of liquid hold-up for a high-voidage structured packing. *Chem. Eng. Sci.* 55 (13), 2401–2415. doi:10.1016/S0009-2509(99)00520-5

Chamchan, N., Chang, J. Y., Hsu, H. C., Kang, J. L., Wong, D. S. H., Jang, S. S., et al. (2017). Comparison of rotating packed bed and packed bed absorber in pilot plant and model simulation for CO2 capture. *J. Taiwan Inst. Chem. Eng.* 73, 20–26. doi:10.1016/j.jtice.2016.08.046

Chandra, A., Goswami, P. S., and Rao, D. P. (2005). Characteristics of flow in a rotating packed bed (HIGEE) with split packing. *Industrial Eng. Chem. Res.* 44 (11), 4051–4060. doi:10.1021/ie048815u

Chen, T. L., Pei, S. L., Pan, S. Y., Yu, C. Y., Chang, C. L., and Chiang, P. C. (2020). An engineering-environmental-economic-energy assessment for integrated air pollutants reduction, CO2 capture and utilization exemplified by the high-gravity process. *J. Environ. Manag.* 255, 109870. doi:10.1016/j.jenvman.2019.109870

Chen, Y. H., Chang, C. Y., Su, W. L., Chen, C. C., Chiu, C. Y., Yu, Y. H., et al. (2004). Modeling ozone contacting process in a rotating packed bed. *Industrial Eng. Chem. Res.* 43 (1), 228–236. doi:10.1021/ie030545c

Chen, Y. S. (2011). Correlations of mass transfer coefficients in a rotating packed bed. *Industrial Eng. Chem. Res.* 50 (3), 1778–1785. doi:10.1021/ie101251z

Chen, Y. S., Lin, C. C., and Liu, H. S. (2005). Mass transfer in a rotating packed bed with various radii of the bed. *Industrial Eng. Chem. Res.* 44 (20), 7868–7875. doi:10.1021/ie048962s

Chen, Y. S., Lin, F. Y., Lin, C. C., Tai, C. Y. der, and Liu, H. S. (2006). Packing characteristics for mass transfer in a rotating packed bed. *Industrial Eng. Chem. Res.* 45 (20), 6846–6853. doi:10.1021/ie060399l

Cheng, H. H., Lai, C. C., and Tan, C. S. (2013). Thermal regeneration of alkanolamine solutions in a rotating packed bed. *Int. J. Greenh. Gas Control* 16, 206–216. doi:10.1016/j.ijggc.2013.03.022

Cheng, H. H., and Tan, C. S. (2009). Carbon dioxide capture by blended alkanolamines in rotating packed bed. *Energy Procedia* 1 (1), 925–932. doi:10.1016/j.egypro.2009.01.123

Chu, G. W., Sang, L., Du, X. K., Luo, Y., Zou, H. K., and Chen, J. F. (2015). Studies of CO2 absorption and effective interfacial area in a two-stage rotating packed bed with nickel foam packing. *Chem. Eng. Process. Process Intensif.* 90, 34–40. doi:10.1016/j.cep.2015.02.007

Cortes Garcia, G. E., van der Schaaf, J., and Kiss, A. A. (2017). A review on process intensification in HiGee distillation. *J. Chem. Technol. Biotechnol.* 92 (6), 1136–1156. doi:10.1002/jctb.5206

Dash, S. K., Parikh, R., and Kaul, D. (2022). Development of efficient absorbent for CO2 capture process based on (AMP + 1MPZ). *Mater. Today Proc.* 62 (P13), 7072–7076. doi:10.1016/j.matpr.2022.01.148

Dash, S. K., Samanta, A. N., and Bandyopadhyay, S. S. (2012). Experimental and theoretical investigation of solubility of carbon dioxide in concentrated aqueous solution of 2-amino-2-methyl-1-propanol and piperazine. *J. Chem. Thermodyn.* 51, 120–125. doi:10.1016/j.jct.2012.02.012

Dey, A., Dash, S. K., and Mandal, B. (2018). Equilibrium CO_2 solubility and thermophysical properties of aqueous blends of 1-(2-aminoethyl) piperazine and N-methyldiethanolamine. *Fluid Phase Equilibria* 463, 91–105. doi:10.1016/j.fluid.2018.01.030

Dey, A., Mandal, B., and Dash, S. K. (2020). Analysis of equilibrium CO_2 solubility in aqueous APDA and its potential blends with AMP/MDEA for postcombustion CO_2 capture. *Int. J. Energy Res.* 44 (15), 12395–12415. doi:10.1002/er.5404

Dhaneesh, K. P., and Ranganathan, P. (2022). A comprehensive review on the hydrodynamics, mass transfer and chemical absorption of CO_2 and modelling aspects of rotating packed bed. *Sep. Purif. Technol.* 295, 121248. doi:10.1016/j.seppur.2022.121248

Esmaeili, A., Tamuzi, A., Borhani, T. N., Xiang, Y., and Shao, L. (2022). Modeling of carbon dioxide absorption by solution of piperazine and methyldiethanolamine in a rotating packed bed. *Chem. Eng. Sci.* 248, 117118. doi:10.1016/j.ces.2021.117118

Gao, X. Y., Liu, L., Hu, M. L., Xiang, Y., Chu, G. W., Zou, H. K., et al. (2016). Numerical simulation for mass transfer characteristics of CO2 capture in a rotating packed bed. *Chem. Eng. Process. Process Intensif.* 109, 68–79. doi:10.1016/j.cep.2016.08.015

Guo, J., Jiao, W., Qi, G., Yuan, Z., and Liu, Y. (2019). Applications of high-gravity technologies in gas purifications: A review. *Chin. J. Chem. Eng.* 27 (6), 1361–1373. doi:10.1016/j.cjche.2019.01.011

Harun, N., Nittaya, T., Douglas, P. L., Croiset, E., and Ricardez-Sandoval, L. A. (2012). Dynamic simulation of MEA absorption process for CO2 capture from power plants. *Int. J. Greenh. Gas Control* 10, 295–309. doi:10.1016/j.ijggc.2012.06.017

Hendry, J. R., Lee, J. G. M., and Attidekou, P. S. (2020). Pressure drop and flooding in rotating packed beds. *Chem. Eng. Process. - Process Intensif.* 151, 107908. doi:10.1016/j.cep.2020.107908

Im, D., Jung, H., and Lee, J. H. (2020). Modeling, simulation and optimization of the rotating packed bed (RPB) absorber and stripper for MEA-based carbon capture. *Comput. Chem. Eng.* 143, 107102. doi:10.1016/j.compchemeng.2020.107102

IPCC (2022). *Climate Change 2022: Impacts, adaptation, and vulnerability. Contribution of working group II to the sixth assessment report of the IPCC.* Cambridge, United Kingdom and New York, NY: Cambridge University Press, 3056. doi:10.1017/9781009325844

Jassim, M. S. (2002). *Process intensification: Absorption and desorption of carbon dioxide from monoethanolamine solutions using higee technology*. Newcastle, England: Newcastle University.

Jassim, M. S., Rochelle, G., Eimer, D., and Ramshaw, C. (2007). Carbon dioxide absorption and desorption in aqueous monoethanolamine solutions in a rotating packed bed. *Industrial Eng. Chem. Res.* 46 (9), 2823–2833. doi:10.1021/ie051104r

Jiao, W. Z., Liu, Y. Z., and Qi, G. S. (2010). Gas pressure drop and mass transfer characteristics in a cross-flow rotating packed bed with porous plate packing. *Industrial Eng. Chem. Res.* 49 (8), 3732–3740. doi:10.1021/ie9009777

Jin, H., Li, J., Liu, P., and Li, Z. (2019). Rate-based modelling and validation of an absorber and stripper in an amine-based post-combustion CO2 capture process. *Chem. Eng. Trans.* 76, 811–816. doi:10.3303/CET1976136

Joel, A. S., Wang, M., and Ramshaw, C. (2015). Modelling and simulation of intensified absorber for post-combustion CO2 capture using different mass transfer correlations. *Appl. Therm. Eng.* 74, 47–53. doi:10.1016/j.applthermaleng.2014.02.064

Joel, A. S., Wang, M., Ramshaw, C., and Oko, E. (2014). Process analysis of intensified absorber for post-combustion CO2 capture through modelling and simulation. *Int. J. Greenh. Gas Control* 21, 91–100. doi:10.1016/j.ijggc.2013.12.005

Kang, J. L., Sun, K., Wong, D. S. H., Jang, S. S., and Tan, C. S. (2014). Modeling studies on absorption of CO2 by monoethanolamine in rotating packed bed. *Int. J. Greenh. Gas Control* 25, 141–150. doi:10.1016/j.ijggc.2014.04.011

Kelleher, T., and Fair, J. R. (1996). Distillation studies in a high-gravity contactor. *Ind. Eng. Chem. Res.* 35 (12), 4646–4655. doi:10.1021/ie950662a

Keyvani, M., and Gardner, N. C. (1989). Operating characteristics of rotating beds. *Chem. Eng. Prog.* 85 (9), 48–52.

Koronaki, I. P., Prentza, L., and Papaefthimiou, V. (2015). Modeling of CO2 capture via chemical absorption processes - an extensive literature review. *Renew. Sustain. Energy Rev.* 50, 547–566. doi:10.1016/j.rser.2015.04.124

Kvamsdal, H. M., Jakobsen, J. P., and Hoff, K. A. (2009). Dynamic modeling and simulation of a CO2 absorber column for post-combustion CO2 capture. *Chem. Eng. Process. Process Intensif.* 48 (1), 135–144. doi:10.1016/j.cep.2008.03.002

Li, H., Li, L., Nguyen, T., Rochelle, G. T., and Chen, J. (2013). Characterization of piperazine/2-aminomethylpropanol for carbon dioxide capture. *Energy Procedia* 37, 340–352. doi:10.1016/j.egypro.2013.05.120

Li, W., Wei, S., Jiao, W., Qi, G., and Liu, Y. (2016). Modelling of adsorption in rotating packed bed using artificial neural networks (ANN). *Chem. Eng. Res. Des.* 114, 89–95. doi:10.1016/j.cherd.2016.08.013

Li, Y., Lu, Y., Liu, X. J., Wang, G., Nie, Y., and Ji, J. (2017). Mass-transfer characteristics in a rotating zigzag bed as a Higee device. *Sep. Purif. Technol.* 186, 156–165. doi:10.1016/j.seppur.2017.05.049

Lin, C. C., and Jian, G. S. (2007). Characteristics of a rotating packed bed equipped with blade packings. *Sep. Purif. Technol.* 54 (1), 51–60. doi:10.1016/j.seppur.2006.08.006

Lin, C. C., and Kuo, Y. W. (2016). Mass transfer performance of rotating packed beds with blade packings in absorption of CO2 into MEA solution. *Int. J. Heat Mass Transf.* 97, 712–718. doi:10.1016/j.ijheatmasstransfer.2016.02.033

Liu, Y., Zhang, F., Gu, D., Qi, G., Jiao, W., and Chen, X. (2016). Gas-phase mass transfer characteristics in a counter airflow shear rotating packed bed. *Can. J. Chem. Eng.* 94 (4), 771–778. doi:10.1002/cjce.22434

Liu, Z. W., Liang, F. N., and Liu, Y. Z. (2018). Artificial neural network modeling of biosorption process using agricultural wastes in a rotating packed bed. *Appl. Therm. Eng.* 140, 95–101. doi:10.1016/j.applthermaleng.2018.05.029

Lockett, M. J. (1995). Flooding of rotating structured packing and its application to conventional packed-columns. *Chem. Eng. Res. Des.* 73, 379–984.

Lu, X., Xie, P., Ingham, D. B., Ma, L., and Pourkashanian, M. (2019). Modelling of CO2 absorption in a rotating packed bed using an Eulerian porous media approach. *Chem. Eng. Sci.* 199, 302–318. doi:10.1016/j.ces.2019.01.029

Luo, Y., Chu, G. W., Zou, H. K., Wang, F., Xiang, Y., Shao, L., et al. (2012a). Mass transfer studies in a rotating packed bed with novel rotors: Chemisorption of CO 2. *Industrial Eng. Chem. Res.* 51 (26), 9164–9172. doi:10.1021/ie300466f

Luo, Y., Chu, G. W., Zou, H. K., Zhao, Z. Q., Dudukovic, M. P., and Chen, J. F. (2012b). Gas-liquid effective interfacial area in a rotating packed bed. *Industrial Eng. Chem. Res.* 51 (50), 16320–16325. doi:10.1021/ie302531j

Luo, Y., Luo, J. Z., Chu, G. W., Zhao, Z. Q., Arowo, M., and Chen, J. F. (2017). Investigation of effective interfacial area in a rotating packed bed with structured stainless steel wire mesh packing. *Chem. Eng. Sci.* 170, 347–354. doi:10.1016/j.ces.2016.10.023

Ma, H. J., and Chen, Y. S. (2016). Evaluation of effectiveness of highly concentrated alkanolamine solutions for capturing CO2 in a rotating packed bed. *Int. J. Greenh. Gas Control* 55, 55–59. doi:10.1016/j.ijggc.2016.11.009

Mallinson, R. H., and Ramshaw, C. (1981). *Mass transfer process*. Patent No. 4,283,255. United States: United States Patent.

Marx-Schubach, T., and Schmitz, G. (2019). Modeling and simulation of the start-up process of coal fired power plants with post-combustion CO2 capture. *Int. J. Greenh. Gas Control* 87, 44–57. doi:10.1016/j.ijggc.2019.05.003

Mohammadi Nouroddinvand, V., and Heidari, A. (2021). Experimental study of CO2 absorption with MEA solution in a novel Arc-RPB. *Chem. Eng. Process. - Process Intensif.* 165, 108450. doi:10.1016/j.cep.2021.108450

Neumann, K., Gladyszewski, K., Groß, K., Qammar, H., Wenzel, D., Górak, A., et al. (2018). A guide on the industrial application of rotating packed beds. *Chem. Eng. Res. Des.* 134, 443–462. doi:10.1016/j.cherd.2018.04.024

Onda, K., Sada, E., and Takeuchi, H. (1968). Gas absorption with chemical reaction in packed columns. *Sammak Trans. Inst. Chem. Engrs* 36 (9), 62–66. doi:10.1252/jcej.1.62

Otitoju, O., Oko, E., and Wang, M. (2023). Modelling, scale-up and techno-economic assessment of rotating packed bed absorber for CO2 capture from a 250 MWe combined cycle gas turbine power plant. *Appl. Energy* 335, 120747. doi:10.1016/j.apenergy.2023.120747

Pan, S. Y., Wang, P., Chen, Q., Jiang, W., Chu, Y. H., and Chiang, P. C. (2017). Development of high-gravity technology for removing particulate and gaseous pollutant emissions: Principles and applications. *J. Clean. Prod.* 149, 540–556. doi:10.1016/j.jclepro.2017.02.108

Pandya, J. D. (1983). Adiabatic gas absorption and stripping with chemical reaction in packed towers. *Chem. Eng. Commun.* 19 (4–6), 343–361. doi:10.1080/00986448308956351

Podbielniak, W. J. (1935). *Centrifugal counter current contact apparatus*. United States: US patent 2,004,011.

Qian, Z., Xu, L., Cao, H., and Guo, K. (2009). Modeling study on absorption of CO2 by aqueous solutions of n-methyldiethanolamine in rotating packed bed. *Industrial Eng. Chem. Res.* 48 (20), 9261–9267. doi:10.1021/ie900894a

Rajan, S., Kumar, M., Ansari, M. J., Rao, D. P., and Kaistha, N. (2011). Limiting gas liquid flows and mass transfer in a novel rotating packed bed (HiGee). *Industrial Eng. Chem. Res.* 50 (2), 986–997. doi:10.1021/ie100899r

Rao, D. P., Bhowal, A., and Goswami, P. S. (2004). Process intensification in rotating packed beds (HIGEE): An appraisal. *Industrial Eng. Chem. Res.* 43 (4), 1150–1162. doi:10.1021/ie030630k

Rao, D. P. (2022). Commentary: Evolution of high gravity (HiGee) technology. *Industrial Eng. Chem. Res.* 61 (2), 997–1003. doi:10.1021/acs.iecr.1c04587

Reay, D. (2008). The role of process intensification in cutting greenhouse gas emissions. *Appl. Therm. Eng.* 28 (16), 2011–2019. doi:10.1016/j.applthermaleng.2008.01.004

Sandilya, P., Rao, D. P., Sharma, A., and Biswas, G. (2001). Gas-phase mass transfer in a centrifugal contactor. *Industrial Eng. Chem. Res.* 40 (1), 384–392. doi:10.1021/ie0000818

Shahid, M. Z., Maulud, A. S., Bustam, M. A., Suleman, H., Abdul Halim, H. N., and Shariff, A. M. (2021). Packed column modelling and experimental evaluation for CO2 absorption using MDEA solution at high pressure and high CO2 concentrations. *J. Nat. Gas Sci. Eng.* 88, 103829. doi:10.1016/j.jngse.2021.103829

Sherwood, T. K., Shipley, A. N. D, G. H., and Holloway, F. A. L. (1938). Flooding velocities in packed columns. *Ind. Eng. Chem.* 30 (7), 765–769. doi:10.1021/ie50343a008

Su, M. J., Luo, Y., Chu, G. W., Liu, W., Zheng, X. H., and Chen, J. F. (2018). Gas-side mass transfer in a rotating packed bed with structured nickel foam packing. *Industrial Eng. Chem. Res.* 57 (13), 4743–4747. doi:10.1021/acs.iecr.8b00269

Sun, B. C., Wang, X. M., Chen, J. M., Chu, G. W., Chen, J. F., and Shao, L. (2009). Simultaneous absorption of CO2 and NH3 into water in a rotating packed bed. *Industrial Eng. Chem. Res.* 48 (24), 11175–11180. doi:10.1021/ie9001316

Tsai, C. Y., and Chen, Y. S. (2015). Effective interfacial area and liquid-side mass transfer coefficients in a rotating bed equipped with baffles. *Sep. Purif. Technol.* 144, 139–145. doi:10.1016/j.seppur.2015.02.008

Tung, H. H., and Mah, R. S. H. (1985). Modeling liquid mass transfer in higee separation process. *Chem. Eng. Commun.* 39 (1–6), 147–153. doi:10.1080/00986448508911667

Wallis, G. B. (1969). *One-dimensional two-phase flow (vol. 243)*. McGraw-Hill.

Wang, M., Joel, A. S., Ramshaw, C., Eimer, D., and Musa, N. M. (2015). Process intensification for post-combustion CO2 capture with chemical absorption: A critical review. *Appl. Energy* 158, 275–291. doi:10.1016/j.apenergy.2015.08.083

Wang, M., Lawal, A., Stephenson, P., Sidders, J., and Ramshaw, C. (2011). Post-combustion CO2 capture with chemical absorption: A state-of-the-art review. *Chem. Eng. Res. Des.* 89 (9), 1609–1624. doi:10.1016/j.cherd.2010.11.005

Wang, Y., Dong, Y., Zhang, L., Chu, G., Zou, H., Sun, B., et al. (2021). Carbon dioxide capture by non-aqueous blend in rotating packed bed reactor: Absorption and desorption investigation. *Sep. Purif. Technol.* 269, 118714. doi:10.1016/j.seppur.2021.118714

Wu, X., Wang, M., Liao, P., Shen, J., and Li, Y. (2020). Solvent-based post-combustion CO2 capture for power plants: A critical review and perspective on dynamic modelling, system identification, process control and flexible operation. *Appl. Energy* 257, 113941. doi:10.1016/j.apenergy.2019.113941

Xie, P., Lu, X., Yang, X., Ingham, D., Ma, L., and Pourkashanian, M. (2017). Characteristics of liquid flow in a rotating packed bed for CO2 capture: A CFD analysis. *Chem. Eng. Sci.* 172, 216–229. doi:10.1016/j.ces.2017.06.040

Yang, W., Wang, Y., Chen, J., and Fei, W. (2010). Computational fluid dynamic simulation of fluid flow in a rotating packed bed. *Chem. Eng. J.* 156 (3), 582–587. doi:10.1016/j.cej.2009.04.013

Yang, Y., Xiang, Y., Chu, G., Zou, H., Luo, Y., Arowo, M., et al. (2015). A noninvasive X-ray technique for determination of liquid holdup in a rotating packed bed. *Chem. Eng. Sci.* 138, 244–255. doi:10.1016/j.ces.2015.07.044

Yi, F., Zou, H. K., Chu, G. W., Shao, L., and Chen, J. F. (2009). Modeling and experimental studies on absorption of CO2 by Benfield solution in rotating packed bed. *Chem. Eng. J.* 145 (3), 377–384. doi:10.1016/j.cej.2008.08.004

Zhan, J., Wang, B., Zhang, L., Sun, B. C., Fu, J., Chu, G. W., et al. (2020). Simultaneous absorption of H2S and CO2 into the MDEA + PZ aqueous solution in a rotating packed bed. *Industrial Eng. Chem. Res.* 59 (17), 8295–8303. doi:10.1021/acs.iecr.9b06437

Zhang, L. L., Wang, J. X., Xiang, Y., Zeng, X. F., and Chen, J. F. (2011). Absorption of carbon dioxide with ionic liquid in a rotating packed bed contactor: Mass transfer study. *Industrial Eng. Chem. Res.* 50 (11), 6957–6964. doi:10.1021/ie1025979

Zhang, R., Zhang, X., Yang, Q., Yu, H., Liang, Z., and Luo, X. (2017). Analysis of the reduction of energy cost by using MEA-MDEA-PZ solvent for post-combustion carbon dioxide capture (PCC). *Appl. Energy* 205, 1002–1011. doi:10.1016/j.apenergy.2017.08.130

Zhao, B., Su, Y., and Tao, W. (2014). Mass transfer performance of CO2 capture in rotating packed bed: Dimensionless modeling and intelligent prediction. *Appl. Energy* 136, 132–142. doi:10.1016/j.apenergy.2014.08.108

Zhao, B., Tao, W., Zhong, M., Su, Y., and Cui, G. (2016). Process, performance and modeling of CO2 capture by chemical absorption using high gravity: A review. *Renew. Sustain. Energy Rev.* 65, 44–56. doi:10.1016/j.rser.2016.06.059

Nomenclature

A_c cross-sectional area (m^2)
AF-1 air flow rate (kmol/s)
a_c centrifugal acceleration ($m/s^{2)}$
a_e effective interfacial area (m^{-1})
a_p' surface area of the 2 mm diameter bead per unit volume of bead (m^{-1})
a_t surface area of packing per unit volume of bead (m^2/m^3)
a_s specific surface area (m^2/m^3)
a axial distance between discs of rotor (m)
c width of square opening (mm)
$c_{g,i}$ molar concentration of component i in gas phase ($kmol/m^3$)
$c_{l,i}$ molar concentration of component i in liquid phase ($kmol/m^3$)
$c_{v,g}$ specific heat capacity in constant volume (kJ/kmolK)
$c_{p,l}$ specific heat capacity in constant pressure (kJ/kmolK)
c_{pg} specific heat capacity of gas phase (J/kmolK)
c_{pl} specific heat capacity of liquid phase (J/kmolK)
$c_{R3N,total}$ total liquid bulk concentration of MDEA ($kmol/m^3$)
D_G diffusion coefficient of gas phase (m^2/s)
D_p nominal size of packing (m)
D_L diffusion coefficient (m^2/s)
$D_{i,L}$ molecular diffusion of all species (m^2/s)
d diameter of stainless-steel fiber (mm)
d_p effective diameter of packing (m)
F_G molar flow rate of gas phase (kmol/s)
F_L molar flow rate of liquid phase (kmol/s)
F_V F-factor = $V_G.\rho_G^{0.5}$ $(kg^{0.5}/m^{0.5}.s)$
f_w wetted resistance coefficient
F-1 liquid flow rate (kmol/s)
G superficial mass velocity of gas (kg/m^2.hr)
G_{N_2} flow rate of N_2 (m^3/s)
g gravitational acceleration (m/s^2)
g_0 characteristic gravitational acceleration (m/s^2)
H Henry's constant for absorption of CO_2 in MDEA ($kPam^3/kmol$)
ΔH_{rxn} heat of reaction (kJ/kmol)
$\Delta H_{vap,i}$ heat of vaporization of i (kJ/kmol)
h axial height of the packing (m)
h_{gl} heat transfer coefficient (kW/m^3K)
K_2 equilibrium constant
K_3 equilibrium constant
K_G overall volumetric mass transfer coefficient $kmol/m^3hr.kPa$
K coefficient of contraction or expansion
k_G gas phase mass transfer coefficient (m/s)
k_L liquid mass transfer coefficient (m/s)
k_{r_i} reaction rate constant of i reaction ($kmol/m^3/s$)
N_i molar flux of component i (mol/m^2 s)
N_{CO_2} absorption rate of CO_2 per unit volume ($mol/m^3/s$)
P total pressure of the system (kPa)
ΔP_0 pressure drop outside the rotor (kPa)
P-1 pressure (kPa)
P-2 gas Pressure (kPa)
Q_g volumetric flow rate of gas (m^3/s)
q_g heat transfer flux in gas phase (W/m^2)
q_l heat transfer flux in liquid phase (W/m^2)
R universal gas constant ($m^3atm/kg.mol.K$)
R_s rotational speed of RPB rpm
r radial coordinate of the packed bed from the center (m)
r_i inner radius (m)
r_0 inner radius (m)
T absolute temperature (K)
T-1 liquid inlet temperature (K)
T-2 gas inlet temperature (K)
T-3 gas cooler temperature (K)
T-4 liquid outlet temperature (K)
T_G gas phase temperature (K)
T_L liquid phase temperature (K)
U_1 liquid superficial velocity (m/s)
U_0 characteristic liquid superficial velocity (m/s)
U_g gas superficial velocity (m/s)
V_0 volume between the outer radius of the bed and the stationary housing (m^3)
V_G average gas superficial velocity (m/s)
V_t total volume of the RPB (m^3)
V_i volume inside the inner radius of the bed (m^3)
x_i mole fraction of component i in liquid phase (mol/mol)
y_i mole fraction of component i in gas phase (mol/mol)

Dimensionless symbols

Fr_L liquid Froude number
Ga galileo number
Gr_G gas Grashof number
Gr_L liquid Grashof number
Re_G gas Reynolds number
Re_L liquid Reynolds number
Sc_L liquid Schmidt number
We_L liquid Weber number

Greek symbols

μ_G viscosity of gas phase (kg/ms)
ρ_G density of gas phase (kg/m^3)

σ_c critical surface tension (kg/s^2)
σ_w surface tension of water (kg/s^2)
σ surface tension (kg/s^2)
ε_g hold up in gas phase (m^3/m^3)
ε_l hold up in liquid phase (m^3/m^3)
ν, ν_g kinematic viscosity (mm^2/s)
ν_0 characteristic Kinematic viscosity (mm^2/s)
γ dynamic contact angle Degree
γ_0 characteristic Dynamic contact angle Degree
ω angular speed rad/s
β constant